energies

Article

Impact of the Application of Fuel and Water Emulsion on CO and NOx Emission and Fuel Consumption in a Miniature Gas Turbine

Paweł Niszczota * and Marian Gieras

Department of Division of Aircraft Engines, Warsaw University of Technology, 00-661 Warsaw, Poland; marian.gieras@itc.pw.edu.pl
* Correspondence: pawel.niszczota.dokt@pw.edu.pl

Abstract: Miniature gas turbines (MGT) are an important part of the production of electric energy in distributed systems. Due to the growing requirements for lower emissions and the increasing prices of hydrocarbon fuels, it is becoming more and more important to enhance the efficiency and improve the quality of the combustion process in gas turbines. One way to reduce NOx emissions is to add water to the fuel in the form of a water-based emulsion (FWE). This article presents the research results and the analysis of the impact of the use of FWE on CO and NOx emissions as well as on fuel consumption in MGT GTM-120. Experimental tests and numerical calculations were carried out using standard fuel (DF) and FWE with water content from 3% to 12%. It was found that the use of FWE leads to a reduction in NOx and CO emissions and reduction in the consumption of basic fuel. The maximum reduction in emissions by 12.32% and 35.16% for CO and NOx, respectively, and a reduction in fuel consumption by 5.46% at the computational operating point of the gas turbine were recorded.

Keywords: miniature gas turbine; combustion zone; CO emissions; NOx emissions; water fuel emulsion; fuel consumption

Citation: Niszczota, P.; Gieras, M. Impact of the Application of Fuel and Water Emulsion on CO and NOx Emission and Fuel Consumption in a Miniature Gas Turbine. *Energies* **2021**, *14*, 2224. https://doi.org/10.3390/en14082224

Academic Editor: Andrea De Pascale

Received: 30 March 2021
Accepted: 13 April 2021
Published: 16 April 2021

1. Introduction

Miniature gas turbines (MGT) are listed as one of the primary ways to produce electricity in distributed systems [1,2]. They are characterized by numerous advantages. In energy applications used in parallel with the electricity network, they increase system reliability, reduce peak load or eliminate the need for a reserve margin [3]. In addition, MGT is characterized by compact size, high power-to-weight ratio and the ability to supply various fuels [4,5]. It can be an important source of energy in areas without access to the central electricity network and in hard-to-reach places [6]. Despite the undoubted advantages of MGT, it has disadvantages, such as relatively low efficiency [7] and high heat loss through the housing [8].

Due to the high potential of MGT and their wide application, numerous studies are being conducted on increasing efficiency and reducing emissions [4,5,9–13]. The works approach the problem from different perspectives and include, among others, design changes of MGT and testing the possibility of using alternative fuels. Experimental studies and numerical calculations have shown that, for example, the use of variable geometry of the turbine stator blades in MGT can lead to a reduction in the specific fuel consumption by 4%, an increase in the unit thrust to 5%, with a simultaneous reduction in NOx and CO emissions [9]. Studies on the use of variable combustion chamber geometry have shown that by controlling the amount of air supplied to the primary zone and the dilution zone of the combustion chamber, the efficiency of the turbine can be increased and the emission of undesirable exhaust components can be reduced [10]. It has been shown in [11] that the simultaneous application of the two above-mentioned modifications to the gas turbine can potentially lead to a twofold increase in the thermal efficiency of MGT at the design operating point. The second line of research aimed at increasing the efficiency and reducing the emission of undesirable combustion products from MGT is the use of alternative fuels as a fuel for gas turbines. In [12], the positive effect of biofuels on efficiency and emissions was demonstrated in comparison with the case in which pure Jet-A fuel was burned. For the mixture of 70% Jet-A fuel, 20% rapeseed and 10% ethanol, NOx emissions were reduced by 16%, thermal efficiency increased by 35% and CO emissions decreased. On the other hand, [13] achieved a 5% reduction in CO emissions and a 2% reduction in NOx and CO2 emissions due to the addition of 10% butanol to the Jet A-1 fuel.

Studies are also being conducted on the effect of using water additive to fuel in the form of FWE. However, most of them concern the combustion of FWE in compression ignition engines, and only a few studies have been carried out on gas turbines. Tests conducted on compression ignition engines clearly show that the use of FWE leads to a reduction in NOx emissions and a lower temperature of the exhaust gases. The influence of the FWE engine power supply on CO emission is not clear. The reviews show cases of both an increase and a decrease in CO emission as a result of the use of water addition to fuel [14–19]. The same applies to research conducted on gas turbines. In [20], a decrease in NOx emissions was recorded with an increase in water content in the FWE, a practically constant temperature at the outlet of the gas turbine and an increase in CO emissions. The increase in CO emissions caused by the addition of water to the fuel was also noted in [21]. In [22], the influence of the use of FWE (up to 5% water addition) on the operating parameters and emissions of the air combustion chamber was investigated. As in [20], the reduction of NOx emissions was achieved, but also of the temperature at the outlet from the combustion chamber and the reduction of CO emissions. Experimental studies do not give a straightforward answer as to the impact of the use of FWE on CO emission and do not explain the reasons for the obtained results of measurements of the amount of carbon monoxide in exhaust gases.

The aim of this work was to investigate the influence of the use of an FWE on the operating parameters and emission of a miniature gas turbine, and to explain the mechanisms that led to the obtained experimental results, regarding CO emissions in particular. Experimental tests were carried out on a miniature gas turbine GTM-120. Four FWE variants with a mass water content from 3% to 12% with a 2% addition of surfactant were tested and the results were compared with those obtained for the base fuel (Jet A-1). In addition, a CFD calculation was performed for each of the tested cases in order to find out about the changes in the combustion process caused by the use of an alternative fuel.

2. Materials and Methods

The test stand of the miniature gas turbine GTM-120 is shown schematically in Figure 1. The MGT test stand allows the measurement of temperatures and pressures in characteristic cross-sections and the composition of exhaust gases in a 5′ cross-section (Figure 1). In the turbine inlet section 2′, static and dynamic pressure as well as total temperature were measured. The static pressure and total temperature were measured in 3′ and 4′ sections.

Fuel consumption was measured using a differential pressure sensor which measured the pressure change exerted by the fuel column during the test. A strain gauge beam was used to measure the thrust. The temperature of the exhaust gases was measured in the 5′ cross-section. For pressure measurement, analog pressure transducers with an internal ceramic diaphragm were used. The temperature was measured with NiCr-NiAl sheathed thermocouples. The fuel consumption measurement was recorded using a differential pressure sensor. All measurement data were recorded using a computer data acquisition system with the possibility of direct observation of changes in individual signals during MGT operation with a frequency of 40 Hz. The exhaust gas composition was measured using a Testo 350 analyzer equipped with electrochemical measuring sensors. In the initial stage of the turbine start-up, it is fed with propane; then, the control system switches the turbine to run on liquid fuel. Originally, the primary fuel was a mixture of Jet A-1 fuel (95%) with AeroShell Turbine 500 oil (5%), which is also used to lubricate the bearings.

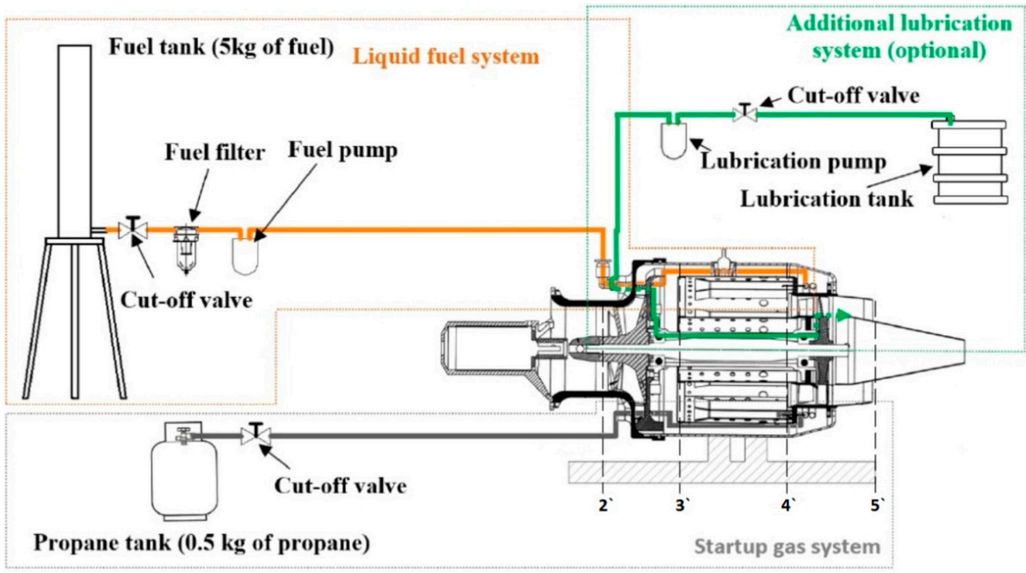

Figure 1. Test stand for the miniature gas turbine GTM-120.

For the purposes of the research, the factory lubrication system of two MGT gas turbine bearings was modified accordingly. Due to the fact that, in the course of the research, ingredients reducing its lubricating properties were added to the standard fuel mixture, it was decided to use a proprietary bearing lubrication system, completely independent of the fuel supply system to the combustion chamber. It consists of an additional fuel tank containing a Jet A-1 mixture with 5% oil additive (DF), a valve and a pump. It has been experimentally checked that the amount of DF supplied to the bearing space through the additional lubrication system does not change the MGT operating parameters and the exhaust gas composition.

The FWE, which was fed with MGT during the experimental tests, is a heterogeneous mixture of fuel and water. In the analyzed case, water is the dispersed phase and the fuel is the continuous phase. Figure 2a shows a microscopic photo of the FWE with water droplets clearly visible. Figure 2b shows the standard fuel mixture, i.e., Jet A-1 with 5% oil. In the emulsion production process, a surfactant was used, whose task was to create a boundary surface between the dispersed water droplets and the fuel in order to increase the stability of the mixture (Figure 2c) [23]. Comparative studies carried out for various percentages of surfactant show that its influence in the amounts used in the conducted tests on the measurement results can be considered negligible. Figure 2d shows a ready-to-use macroemulsion with a water content of 6% with a 2% addition of surfactant. In order to obtain the highest possible repeatability of the burnt emulsion, it was prepared not earlier than 30 min before the start of each test. The developed process of preparing the FWE required minimum energy expenditure.

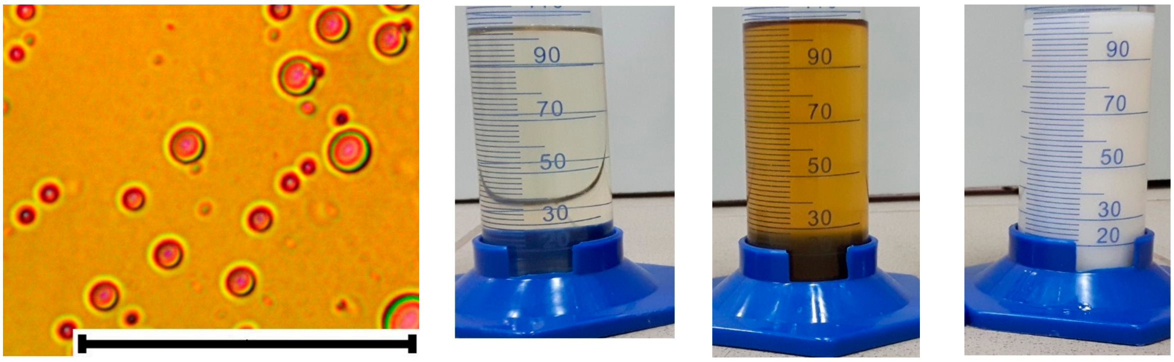

(a) (b) (c) (d)

Figure 2. Fuel–water emulsion: (**a**) FEW microscope photo, scale bar corresponds to 50 µm; (**b**) DF; (**c**) a surfactant; (**d**) FWE with 6% water and 2% surfactant.

3. Experimental Research

Forty-two experimental trials were conducted for five fuel configurations in total. The tests were carried out in two research series. The same MGT operating parameters were measured in both test series. In the first series, tests were carried out for five fuel configurations: default fuel (DF) and four FWE variants. Six tests were performed for each tested variant. The tests of the first series were carried out at the ambient pressure in the range of 983 ÷ 1007 hPa and at the temperature of +18 °C ÷ +23 °C. In the second series, tests were carried out for DF and FWE with 3% water content. Six trials were carried out for each of the two variants. The tests were carried out at a pressure of 987 ÷ 1010 hPa and a temperature of +19.8 °C ÷ +20.7 °C. The composition of the fuel blends used in the research is presented in Table 1. It was decided to carry out tests for FWE with a water content in the range of 3% ÷ 12%, as this is the range that allows reduction of NOx emissions without reducing the thermal efficiency of the gas turbine. Thus, this is the scope in which the application of the FWE has an economic rationale. This is confirmed by a study carried out on full-size gas turbines, which showed that the range of 5% ÷ 15% water content in the FWE is optimal [24]. Based on the tests carried out for 2.5% and 5% water content in the FWE, it was found that reducing the water content to 2.5% in the FWE gives the best results in terms of reducing emissions and maintaining efficiency [22].

Table 1. Percentage of ingredients in the fuel mixture (by weight).

Fuel Mixture	Jet A-1	Oil	Surfactant	Water
Default fuel	95.00	5.00	0	0
3% Fuel–Water Emulsion	90.25	4.75	2	3
6% Fuel–Water Emulsion	87.40	4.60	2	6
9% Fuel–Water Emulsion	84.55	4.45	2	9
12% Fuel–Water Emulsion	81.70	4.30	2	12

All the experiments in each of the two series of tests were carried out in an identical manner according to the procedure described below. The MGT was started in an automatic mode. In the initial phase of this process, propane was fed to the combustion chamber in order to ensure that the temperature of the combustion chamber enabled the liquid fuel to evaporate quickly enough. After these conditions were achieved, feeding to the DF combustion chamber was started, and the gas supply was cut off. The automatic start-up process is completed when the speed reaches 33 k rpm and the MGT enters the manual control mode. In the conducted tests, the speed of 40 k rpm was adopted as the first measuring point. After reaching the set rotational speed, the operating parameters and the composition of exhaust gases were recorded for 120 s. After this time, the engine speed was increased by 20 k rpm, all the way to 120 k rpm, each time leaving the MGT at the given rpm for 120 s. The accuracy of the speed control for the 40 k ÷ 100 k rpm range was ±600 rpm, while, for the measuring point, it was 120 k rpm, +0 rpm ÷ −10 k rpm. During each of the experimental tests, pressure and temperature courses were recorded in the given cross-section measurement planes. Moreover, the composition of exhaust gases (NO, NO2, CO) was determined and the engine thrust and fuel consumption were measured. Before the commencement of each of the two test series, all sensors and the test stand were secured against moving. This was especially true of thermocouples, for which even a slight change in position can significantly change the temperature reading. The sensors of the exhaust gas analyzer, before starting the tests, were calibrated by the manufacturer of the apparatus. The correctness of indications of other sensors was checked by comparing their indications with the indications of reference sensors.

Results of Experimental Research

Figure 3 shows the consumption of FWE and DF depending on the thrust in a miniature gas turbine. The standard deviation for each data point in this and other graphs is denoted the by bars. Measurement accuracy is not shown in the graphs. Detailed discussion on the measurement accuracy for each of the measured values is performed and presented in [10]. It can be seen that the consumption of FWE with increasing water content in the mixture increases for all tested variants (Figure 3a). However, after deducting the water contained in the FWE (in the tested range from 3% to 12%), the DF consumption for all measuring points is lower than in the case of the unmodified DF fuel mixture without the addition of water (Figure 3b).

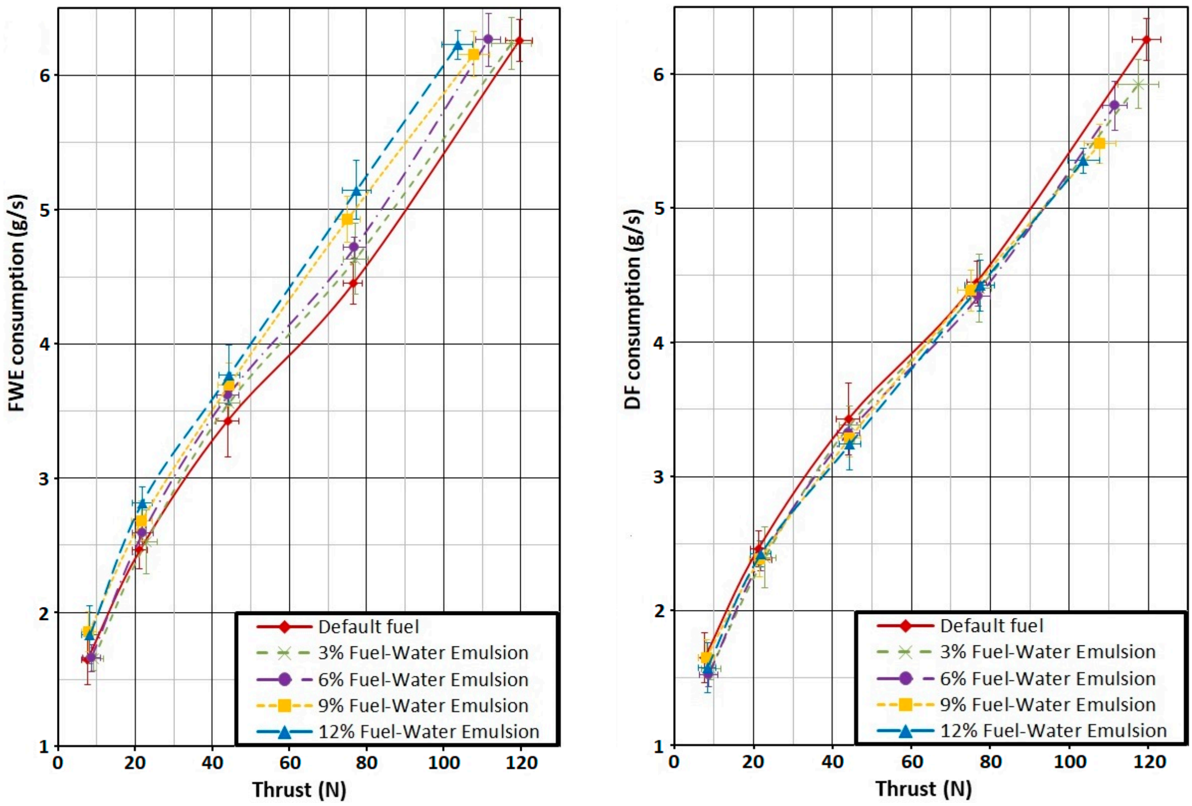

(**a**) (**b**)

Figure 3. Comparison of default fuel and FWE: (**a**) FWE consumption; (**b**) DF consumption.

For example, at a measuring point for a speed of 80 k rpm (thrust value approx. 45 N), which is the design MGT operating point [25], the decrease in DF consumption with an increase in water content from 3% to 12% in FWE is successively 1.28%, 2.94%, 4.1% and 5.46% in relation to DF without the addition of water.

The reduction in the maximum thrust of the GTM-120 turbine, visible in Figure 3, in the case of using FWE, is not caused by the negative effect of the addition of water to the fuel. This is due to the fact that the maximum volume of liquid pumped by the fuel pump is determined for the volume DF.

Figure 4 shows the positive effect of FWE on NOx emissions. The reported NOx emission values are the sum of the measured NO and NO2 emissions. For the maximum achieved thrust, a decrease in NOx emissions by 35.16% was achieved, for a 12% water content in the FWE. However, for the turbine operating point (80 k rpm), the decrease was 17.86% for the same water content in the emulsion. The reduction in NOx emissions with increasing water content in the FWE is due to the extinction of "hot spots" in the primary combustion zone [26,27]. Most of the NO in a gas turbine is produced according to the thermal Zeldovich mechanism [28]. The production of NO in the primary combustion zone is exponentially temperature-dependent, whereby a slight reduction in temperature in the hottest area leads to a significant reduction in thermal NO production—resulting in a reduction in overall NOx emissions. The consequence of reducing the maximum temperature in the combustion chamber is a slight decrease in the average temperature at the outlet from the combustion chamber (Figure 5).

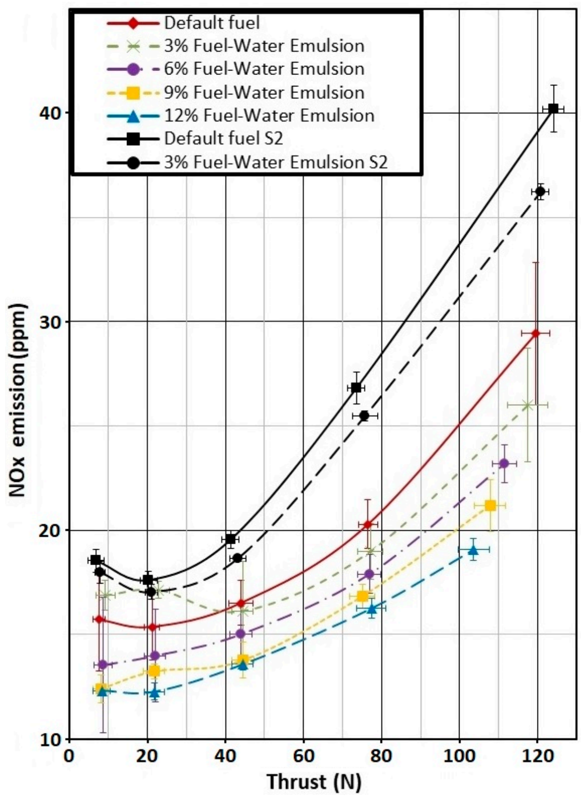

Figure 4. NOx emissions as a function of thrust for different amounts of water in the FWE.

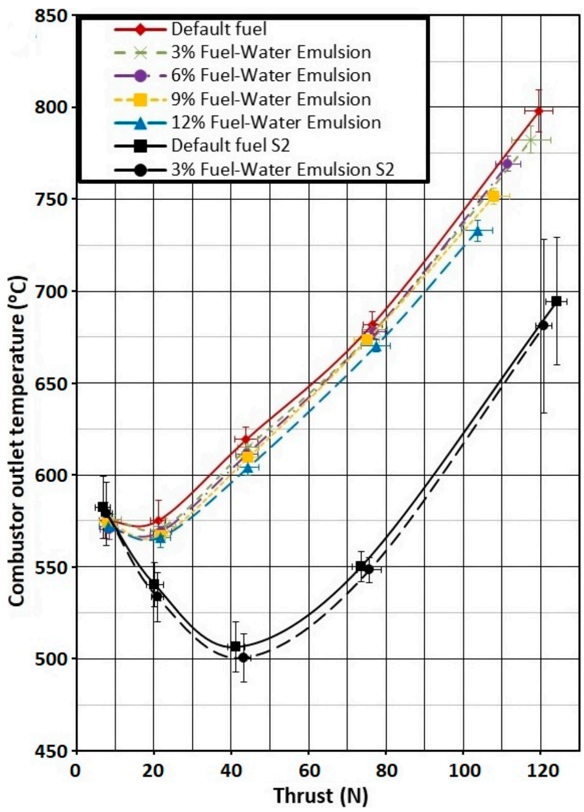

Figure 5. Combustion chamber outlet temperature as a function of thrust for different content of water in the FWE.

In Figure 4, it can be seen that at the measuring points 40 k rpm and 60 k rpm for 3% water content in the few, the results deviate from the general trend of reducing NOx emissions with increasing water content in the FWE. The fact is that for such a low water content (3%), the temperature changes caused by the use of FWE for all measuring points were relatively small. For example, for the measurement point of 100 k rpm and 3% water content in the FWE, a temperature drop after the combustion chamber by 0.45% was recorded. Therefore, in order to verify these results, it was decided to conduct an additional series of experimental tests covering cases in which MGT was fed with DF and FWE with 3% water content. In this series of tests, the position of the exhaust gas analyzer probe and the depth of the thermocouple measuring the temperature behind the combustion chamber were slightly changed. The results of additional tests are shown in Figures 4 and 5 (marked in the legend with "S2"). As can be seen, the second series of tests confirmed the decrease in the temperature behind the combustion chamber in the case of using FWE compared to the combustion of DF. NOx emissions were also recorded following the general trend for the first series of tests; therefore, the results of measuring NOx emissions for the two previously mentioned measuring points can be considered as a local characteristic of turbulent flow of the medium, which does not have to be representative for this flow.

The conducted research shows that the use of water addition to fuel in the form of an FWE reduces CO emissions (Figure 6). The maximum reduction in CO emission was obtained for 60 k rpm and 12% water addition; it is 12.32%. On the other hand, for 80 k rpm, a reduction in CO emission by 7.2% was achieved. Carbon monoxide oxidizes to CO2 relatively slowly. The intensity of this process is positively influenced by the increase in the particle residence time in the primary combustion zone and the increase in temperature. Therefore, one of the main reasons for the increase in CO emissions is areas of reduced temperature, e.g., zones close to the cooled walls of the combustion chamber, where the process of further oxidation to CO2 slows down [29,30]. Due to the negative correlation between CO and NOx emissions, lowering the temperature in the primary combustion zone, which reduces NOx (Figure 4), should also lead to an increase in CO emissions [29]. In the described case, the emissions of NOx and CO were reduced simultaneously, which is an "apparent" contradiction to this rule. It can be assumed that in this case, the combustion of the FWE leads, among others, to the intensification of the fuel-oxidant mixing process and, consequently, to the combustion of a more homogeneous mixture without areas of increased (NOx emission increase) and lowered temperature (CO emission increase).

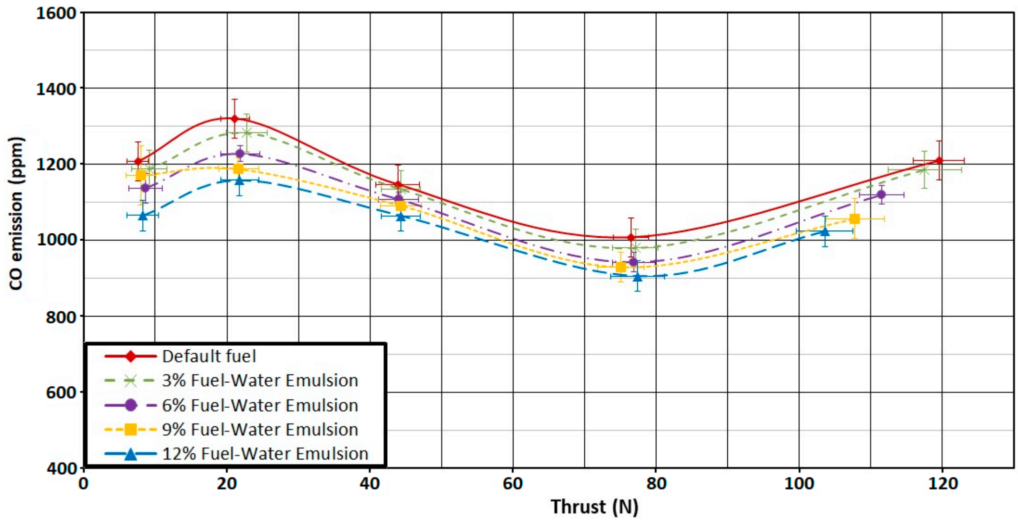

Figure 6. CO emissions as a function of thrust for different content of water in the FWE.

4. Numerical Modeling

The numerical model of the reactive flow through the GTM-120 turbine was created in order to better understand the changes taking place in the combustion process due to the addition of water to the fuel in the form of FWE. The model geometry used for numerical calculations has been simplified. For the purposes of numerical calculations, the moving parts of the engine were omitted. The computing domain starts at the inlet to the compressor diffuser and ends after the turbine stator vanes. Moreover, it was decided to extend the outlet from the engine in order to avoid possible disturbances (Figure 7). This method of simplifying geometry for the purposes of calculations is consistent with [31–33].

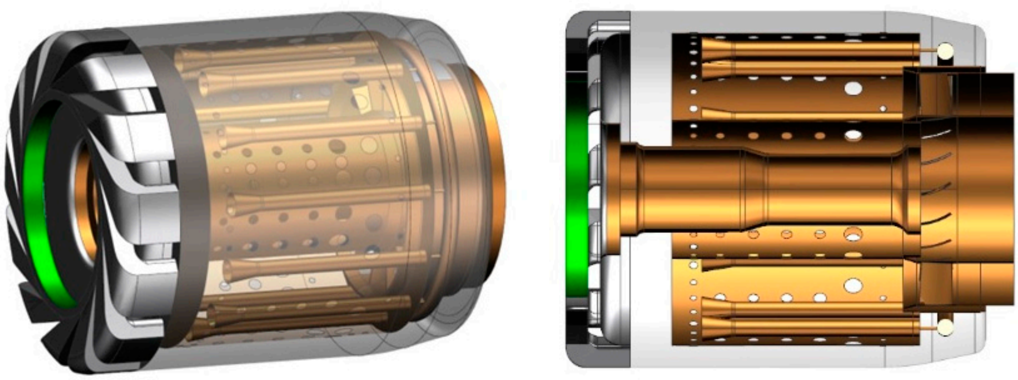

Figure 7. Simplified model of the MGT geometry.

The computation grid is composed of 2.5 M cells. It consists of tetrahedral elements with compaction with prismatic elements near the walls. For a more accurate representation of the wall flow, the size of the boundary layer cells was selected (iteratively) so that the dimensionless distance from the wall y^+ was within the range appropriate for the turbulence model used. The maximum speed in the combustion chamber was used as a parameter with which the influence of the mesh size on the calculation results was tested.

Reducing the number of mesh elements by 20% generates differences in the observed parameter not exceeding 1%. This method of creating a computational mesh is consistent with [27,34].

Numerical calculations were performed using ANSYS Fluent 15. The k-ε turbulence model with the Scalable Wall Function was used in the calculations. The model for heat transport through radiation was the Discrete Ordinates Model. Calculation of the combustion process was performed as a Non-Premixed Combustion model using the Steady Diffusion Flamelet Model. DF and FWE injection were modeled as a Discrete Phase Model. The thermal conditions on the walls of the combustion chamber and evaporators were modeled as coupled two-sided walls.

Numerical simulations were carried out for the boundary conditions corresponding to the operating conditions of the turbine for rotational speeds of 40 k, 60 k, 80 k and 100 k rpm. The calculations were performed for the combustion of DF and FWE with a water content of 3%, 6%, 9% and 12%. Boundary conditions were adopted based on the results of experimental studies from the first series, individually for each of the twenty cases. The mass flow of air at the inlet to the engine was calculated on the basis of the knowledge of dynamic pressure, static pressure and total temperature in the inlet section. In addition, the resultant vector of the inlet air flow direction was entered in a cylindrical configuration based on the velocity triangles at the outlet of the compressor centrifugal rotor. DF and water mass expenditure were set according to the results of experimental studies (Figure 3). The pressure at the outlet from the computational domain was iteratively selected in such a way that the pressure values behind the compressor and the combustion chamber corresponded to the values obtained in the experiment. The solver settings remained unchanged from those described in [27].

Results of Numerical Calculations

The conducted numerical simulations show that adding water to the fuel in the form of a water–fuel emulsion reduces the maximum temperature in the area of the primary combustion chamber, which is consistent with [26,27]. This phenomenon is more intense when there is more water in the FWE (Figure 8). At the same time, the presence of water in the combustion chamber enlarges the area where the temperatures exceed 1300 K. This area widens not only towards the exit from the combustion chamber in the central part of the liner, but also along the walls of the liner, which leads to an increase in the average temperature of these walls (Figure 9). The maximum increase, by 11 K, in the mean wall temperature was recorded for 100 k rpm and 12% water content in the FWE. Generally, it can be concluded that with increasing water content in the FWE (within a given range), the temperature in the primary combustion zone becomes more even and, at the same time, the area in which the temperature value exceeds 1300 K increases.

OH radicals are assumed to be markers of an active reaction zone and are used to identify the area where combustion takes place [35,36]. In Figure 10, it can be seen that the use of FWE in MGT leads to a reduction in the intensity of the chemical reaction in the combustion zone located near the front of the chamber. At the same time, an increased presence of OH radicals is observed in the central part of the combustion chamber, which explains the expansion of the high-temperature region towards the outlet (Figure 8). The use of FWE also increases the intensity of the reaction near the liner walls, increasing their average temperature (Figure 9).

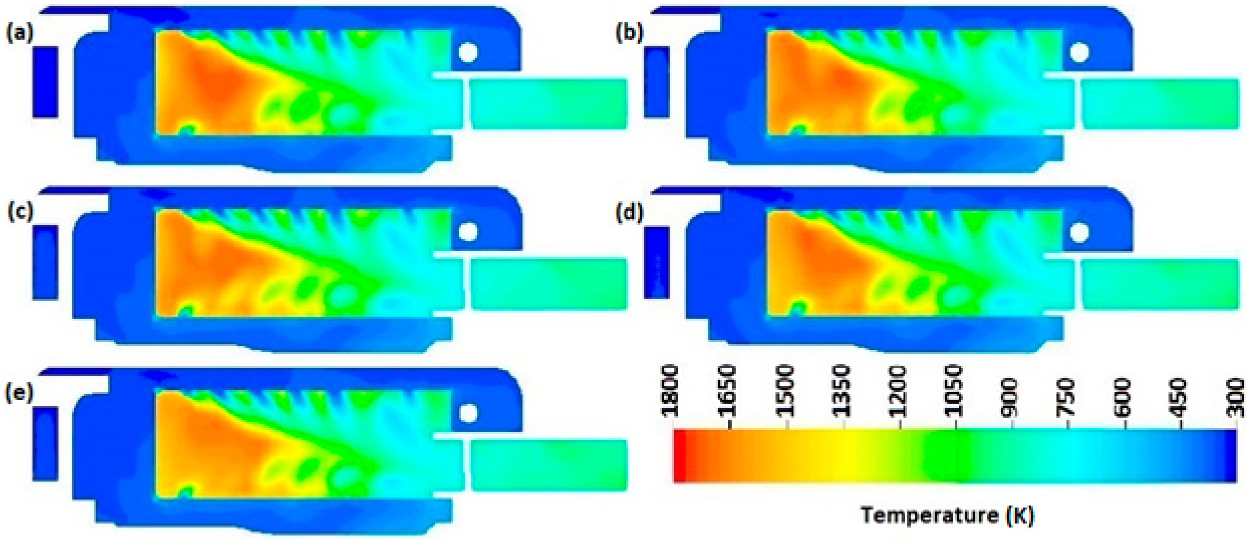

Figure 8. Temperature distribution inside the combustion chamber (60 k rpm): (**a**) DF; (**b**) 3% FWE; (**c**) 6% FWE; (**d**) 9% FWE; (**e**) 12% FWE.

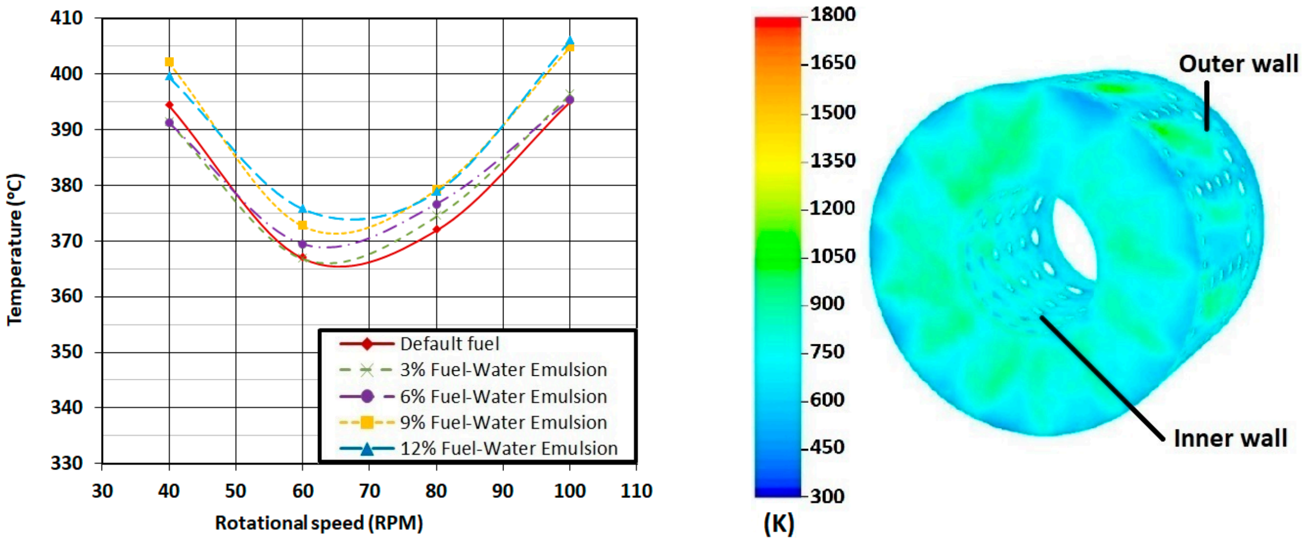

(**a**) (**b**)

Figure 9. Liner wall temperature: (**a**) the average temperature of outer wall and inner wall; (**b**) temperature distribution across the liner walls (3D numerical simulation).

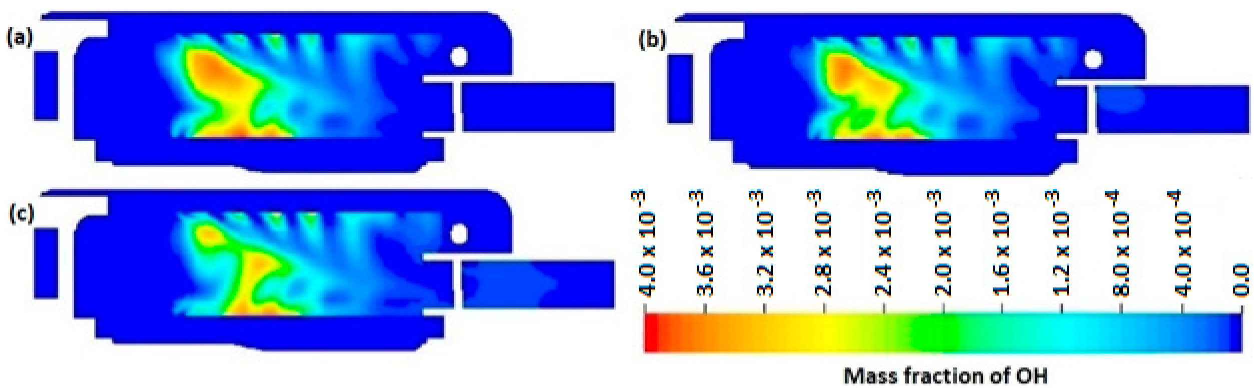

Figure 10. Contours of mass fraction of OH for 100 k rpm: (**a**) DF; (**b**) 6% FWE; (**c**) 12% FWE.

5. Discussion

Experimental studies carried out in the miniature gas turbine GTM-120 have shown that the addition of water to the fuel in the form of FWE leads to a simultaneous reduction in NOx and CO emissions. The reduction in NOx emissions is due to the extinction of the "hot micro-areas" in the primary combustion zone. The production of thermal NO, according to the Zeldovich theory, depends exponentially on the temperature; therefore, lowering the temperature in the areas with maximum values leads to a significant reduction in the formation of nitrogen monoxides and, as a result, contributes to the reduction of NOx emissions [20]. The reduction of NOx emissions was observed for all tested water contents in the FWE. The NOx reduction mechanism has been described in detail for the 3% water content of the FWE in [27]. The research carried out at MGT also shows that the use of FWE contributes to the reduction of CO emissions (compared to DF) for all measuring points, although, as a result of the reduction of the maximum temperature in the main part of the primary combustion zone, an increase in CO emissions could be expected (Figure 11) [37].

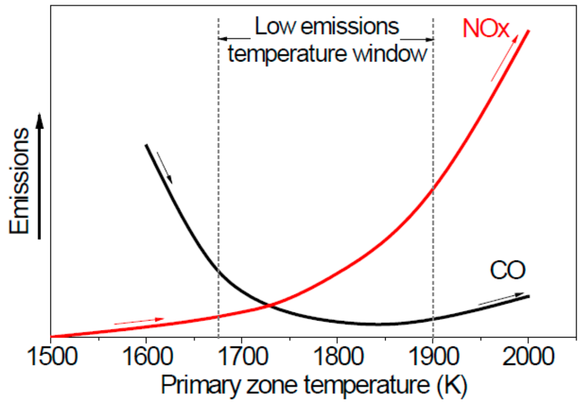

Figure 11. Influence of primary-zone temperature on CO and NOx emission.

Research on the impact of the use of FWE on CO emissions in various combustion engines does not give a clear answer regarding its impact on CO emissions. In compression-ignition reciprocating engines, both an increase and a decrease in CO emissions were achieved after the application of FWE [14–19]. Research conducted in gas turbines also does not clearly define the influence of the use of FWE on CO emissions. In [20,21], the negative impact of the FWE application on CO emission was noted, while in [22], the reduction of carbon monoxide was achieved. The oxidation of CO to CO2 largely proceeds according to the following reaction:

$$CO + OH \leftrightarrow CO2 + H, \quad (1)$$

Reaction (1) at the temperature above 1270 K is of dominant importance in the oxidation of CO [29]. Extension of the area in the combustion chamber of the tested MTE, where the temperature exceeds 1300 K, leads to an increase in the residence time of CO particles in this area and thus extends the duration of this reaction. In the studied range of changes in the water content in the fuel, this area increases with the increase in the water content in the FWE (Figure 8), and, therefore, despite the reduction of the maximum temperature in the primary combustion zone, the degree of CO oxidation taking place in accordance with reaction (1) increases. At lower temperatures, the dominant role in the oxidation of CO to CO2 is played by the reaction [29]:

$$CO + H2O \leftrightarrow CO2 + H2, \quad (2)$$

The addition of water to the fuel increases the amount of H2O molecules in the combustion zone, especially in the middle and rear parts of the combustion chamber

(Figure 12), creating favorable conditions for the oxidation process in these zones, in accordance with reaction (2).

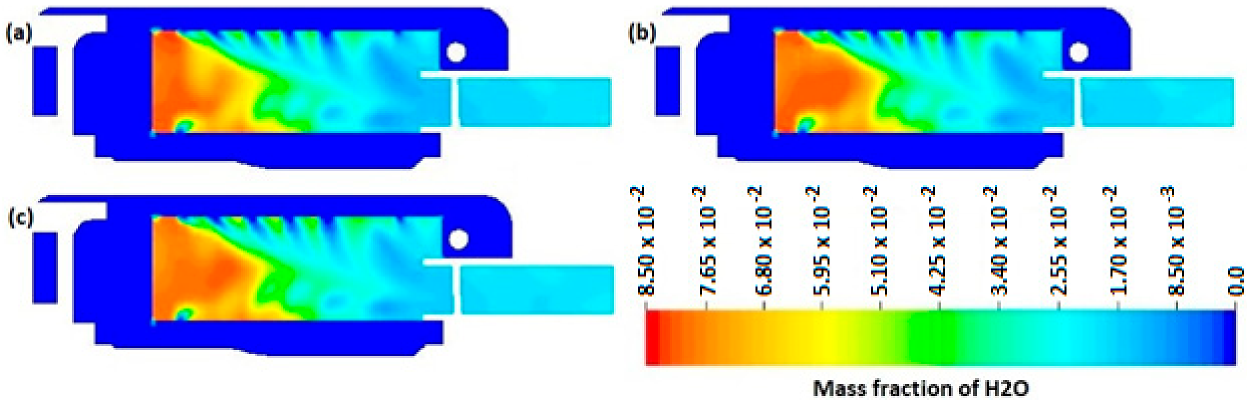

Figure 12. Contours of mass fraction of H2O for 80 k rpm: (**a**) DF; (**b**) 6% FWE; (**c**) 12% FWE.

The contact of CO particles with the cool walls of the liner causes the process of oxidation of CO to CO2 to freeze. This is due to the reduction in the enthalpy of the medium while staying near the cool walls. This effect is observed in both reciprocating engines [30] and gas turbines [38].

The performed numerical calculations showed a tendency to increase the average temperature of the liner walls of the GTM-120 turbine with increasing water content in the FWE (Figure 9). The maximum temperature increase in relation to the case in which the turbine was powered by DF was 11 K. According to [38], an increase in the wall temperature may also have a certain effect on the reduction of CO emissions. The conducted numerical simulations also show that the use of FWE in MGT leads to a reduction in the maximum temperature in local micro-zones, which favors the formation of a more uniform temperature distribution and expansion of the area with increased temperature (Figure 8). Lowering the local maximum combustion temperature results in a reduction in the rate of the chemical reaction, the rate of which is exponentially temperature-dependent. The increased population of OH radicals in the central zone of the combustion chamber, shown in Figure 10, correctly correlates with the temperature distribution. The decrease in the intensity of the reaction in the case of using FWE compared to DF is also observed in the studies of burning single emulsion droplets [39]. Carbon monoxide in the combustion chamber of a gas turbine is formed in areas with local "enrichment" of the mixture. One of the reasons for such spots is that the fuel is applied to the combustion chamber in a way that prevents the fuel from mixing quickly enough with the oxidant. In order to avoid such spots, it is necessary to increase the fragmentation of the droplets injected into the combustion chamber and allow them to premix with the oxidant. In compression-ignition engines, a reduction in CO emissions is observed with increasing fuel injection pressure [40]. Increasing the injection pressure leads to a reduction in the Sauter mean diameter (SMD) of fuel droplets and, as a consequence, it increases the homogenization of the fuel and oxidant mixture and leads to a reduction in CO emissions [41].

Combustion FWE is accompanied by micro-explosion and puffing phenomena, which lead to increased atomization of fuel droplets [42–45]. The occurrence of these phenomena results in better mixing of the burst fuel droplets with air, which reduces the occurrence of locally rich zones. In addition, the broken fuel droplets are characterized by a larger evaporation surface, which should shorten the combustion process. In order to illustrate this process, an experiment was carried out in which a droplet of Jet-A1 fuel emulsion with water with a diameter of approx. 1 mm, suspended on a quartz needle, was quickly immersed in a stream of flowing hot exhaust gas at a temperature of approx. 1200 K. The course of the droplet combustion process is shown in Figure 13. It can be seen that the combustion process of emulsion droplets ends with its violent explosion and intensification of the combustion process of the emulsion micro-droplets formed after the explosion.

Figure 13. Subsequent frames of the film presenting the process of burning a drop of fuel–water emulsion in a stream of hot exhaust gases. Droplet diameter approx. 1 mm. Exhaust gas temperature approx. 1200 K. Filming speed 50 fps.

It is worth noting that the use of FWE (in terms of the tested water concentrations) also solves the problem of corrosion. Since the water is supplied to the engine inside the fuel droplets, there is no direct contact between the metal and the liquid water.

6. Conclusions

The conducted experimental and numerical tests show that the use of FWE as a fuel can significantly reduce NOx and CO emissions, as well as reduce fuel consumption in MGT. It was found that the reduction of NOx emissions is greater when there is more water in the FWE (in the range of 3% ÷ 12% of the water in the FWE). The maximum reduction in NOx emission was recorded for the measuring point corresponding to 120 k rpm and 12% of the water content in the FWE; it was 35.16%, compared to the case in which the MGT was powered by the DF.

The use of FWE in MGT also leads to a reduction in CO emissions. It was observed for all water contents in FWE and for all tested steady states of the engine with respect to DF. The maximum reduction in CO that was recorded was 12.32% for the measuring point corresponding to 60 k rpm and 12% of the water content in the FWE. At the operating point of the GTM-120 turbine (80 k rpm), a simultaneous reduction in NOx and CO emissions was achieved by 17.86% and 7.2%, respectively.

In addition, it was found that the use of FWE in the tested range of water content in fuel leads to a reduction in DF consumption. At the engine operating point corresponding to 80 k rpm, a reduction in DF consumption by 5.46% was recorded for the 12% water content in the FWE. The FWE mass burned by the engine at all measuring points is greater than the fuel mass burned in the base case.

Numerical calculations of the flow and combustion process in the MGT showed a decrease in the maximum temperature in the combustion chamber as a result of the use of FWE. In addition, the use of FWE contributes to the expansion of the primary combustion zone and the reduction of temperature gradients inside the combustion chamber. This is due to the formation of a more homogeneous, better mixed mixture in which the combustion process takes place more evenly. As a result of changes in the temperature distribution in the combustion chamber due to the use of FWE, the average temperature of the walls of the combustion chamber liner slightly increases.

Author Contributions: Conceptualization, M.G. and P.N.; methodology, M.G.; software, P.N.; validation, P.N.; formal analysis, P.N.; investigation, P.N.; resources, M.G. and P.N.; data curation, P.N.; writing—original draft preparation, P.N. and M.G.; writing—review and editing, M.G.; visualization, P.N.; supervision, M.G.; project administration, M.G. and P.N.; funding acquisition, M.G. and P.N. All authors have read and agreed to the published version of the manuscript.

Funding: This research received no external funding.

Acknowledgments: This research was supported by the Faculty of Power and Aeronautical Engineering, Warsaw University of Technology (equipment and materials used for experiments).

Conflicts of Interest: The authors declare no conflict of interest. The funders had no role in the design of the study; in the collection, analyses, or interpretation of data; in the writing of the manuscript, or in the decision to publish the results.

References

1. Zobaa, A.; Cecati, C. A comprehensive review on distributed power generation. In Proceedings of the 2006 International Symposium on Power Electronics, Electrical Drives, Automation and Motion (SPEEDAM 2006), Taormina, Italy, 23–26 May 2006; Institute of Electrical and Electronics Engineers (IEEE): Piscataway, NJ, USA, 2006; pp. 514–518.
2. Chang, L.; Kojabadi, H.M. Review of interconnection standards for distributed power generation. In Proceedings of the LESCOPE'02—2002 Large Engineering Systems Conference on Power Engineering, Halifax, NS, Canada, 26–28 June 2002; Institute of Electrical and Electronics Engineers (IEEE): Piscataway, NJ, USA, 2003.
3. Hofmeester, N.; Bosch, P.V.D. High frequency cycloconverter control. In Proceedings of the 1994 Power Electronics Specialist Conference—PESC'94, Taipei, Taiwan, 20–25 June 1994; Institute of Electrical and Electronics Engineers (IEEE): Piscataway, NJ, USA, 2002.
4. Pilavachi, P. Mini- and micro-gas turbines for combined heat and power. *Appl. Therm. Eng.* **2002**, *22*, 2003–2014. [CrossRef]
5. Gieras, M. *Miniaturowe Silniki Turboodrzutowe*, 1st ed.; Oficyna Wydawnicza Politechniki Warszawskiej: Warsaw, Poland, 2016; pp. 29–51. ISBN 978-83-7814-552-3.
6. Kosoi, A.S.; Popel', O.S.; Beschastnykh, V.N.; Zeigarnik, Y.A.; Sinkevich, M.V. Small gas-turbine units for the power industry: Ways for improving the efficiency and the scale of implementation. *Therm. Eng.* **2017**, *64*, 723–728. [CrossRef]
7. Decuypere, R.; Verstraete, D. *Micro Turbines from the Standpoint of Potential Users*; VKI LS on Micro Gas Turbines: Neuilly-sur-Seine, France, 2005.
8. Verstraete, D.; Bowkett, C. Impact of heat transfer on the performance of micro gas turbines. *Appl. Energy* **2015**, *138*, 445–449. [CrossRef]
9. Fulara, S.; Chmielewski, M.; Gieras, M. Experimental research of the small gas turbine with variable area nozzle. *Proc. Inst. Mech. Eng. Part. G J. Aerosp. Eng.* **2019**, *233*, 5650–5659. [CrossRef]
10. Chmielewski, M. Badanie Wpływu Zmiennej Geometrii Komory Spalania Na Efektywność Procesów Spalania I Emisję Substancji Szkodliwych W Miniaturowej Turbinie Gazowej. Ph.D. Thesis, The Institute of Heat Engineering, Warsaw, Poland, 2016.
11. Fulara, S.; Chmielewski, M.; Gieras, M. Variable Geometry in Miniature Gas Turbine for Improved Performance and Reduced Environmental Impact. *Energies* **2020**, *13*, 5230. [CrossRef]
12. Manigandan, S.; Atabani, A.; Ponnusamy, V.K.; Gunasekar, P. Impact of additives in Jet-A fuel blends on combustion, emission and exergetic analysis using a micro-gas turbine engine. *Fuel* **2020**, *276*, 118104. [CrossRef]
13. Gawron, B.; Białecki, T.; Dzięgielewski, W.; Kaźmierczak, U. Performance and emission characteristic of miniature turbojet engine FED Jet A-1/alcohol blend. *J. KONES* **2016**, *23*, 123–129. [CrossRef]
14. Hasannuddin, A.K.; Wira, J.Y.; Srithar, R.; Sarah, S.; Ahmad, M.I.; Aizam, S.A.; Aiman, M.A.B.; Zahari, M.; Watanabe, S.; Azrin, M.A.; et al. Effect of emulsion fuel on engine emissions—A review. *Clean Technol. Environ. Policy* **2016**, *18*, 17–32. [CrossRef]
15. Jhalani, A.; Sharma, D.; Soni, S.L.; Sharma, P.K.; Sharma, S. A comprehensive review on water-emulsified diesel fuel: Chemistry, engine performance and exhaust emissions. *Environ. Sci. Pollut. Res.* **2019**, *26*, 4570–4587. [CrossRef]
16. Mondal, P.K.; Mandal, B.K. A comprehensive review on the feasibility of using water emulsified diesel as a CI engine fuel. *Fuel* **2019**, *237*, 937–960. [CrossRef]
17. Khan, M.Y.; Karim, Z.A.A.; Hagos, F.Y.; Aziz, A.R.A.; Tan, I.M. Current Trends in Water-in-Diesel Emulsion as a Fuel. *Sci. World J.* **2014**, *2014*, 527472. [CrossRef]
18. Abdollahi, M.; Ghobadian, B.; Najafi, G.; Hoseini, S.; Mofijur, M.; Mazlan, M. Impact of water—biodiesel—diesel nano-emulsion fuel on performance parameters and diesel engine emission. *Fuel* **2020**, *280*, 118576. [CrossRef]
19. Vellaiyan, S.; Amirthagadeswaran, K.S. Emission characteristics of water-emulsified diesel fuel at optimized engine operation condition. *Pet. Sci. Technol.* **2017**, *35*, 1355–1363. [CrossRef]
20. Zhang, Z.; Gollahalli, S.R. Combustion of Kerosene-Water Emulsions in a Gas Turbine Combustor. Turbo Expo: Power for Land, Sea, and Air. *Am. Soc. Mech. Eng.* **1985**, *79436*, V002T04A030. [CrossRef]
21. Moses, C.A.; Coon, C.W.; Altavilla, P.A. *Reduction of Exhaust Smoke from Gas-Turbine Engines by Using Fuel Emulsions*; Southwest Research Institute, Army Fuels and Lubricants Research Lab: San Antonio, TX, USA, 1980.
22. De Giorgi, M.G.; Fontanarosa, D.; Ficarella, A.; Pescini, E. Effects on performance, combustion and pollutants of water emulsified fuel in an aeroengine combustor. *Appl. Energy* **2020**, *260*, 114263. [CrossRef]
23. Sartomo, A.; Santoso, B.; Muraza, O. Recent progress on mixing technology for water-emulsion fuel: A review. *Energy Convers. Manag.* **2020**, *213*, 112817. [CrossRef]
24. Spadaccini, L.J.; Pelmas, R. Evaluation of oil/water emulsion for application in gas turbines. In Proceedings of the Symposium on Evaporation-Combustion of Fuel Droplets, American Chemical Society, DIV. of Petroleum Chem, San Francisco Meeting, San Francisco, CA, USA, 29 August–3 September 1976.
25. Chmielewski, M.; Gieras, M. Small gas turbine GTM-120 bench testing with emission measurements. *J. KONES* **2015**, *22*, 47–54. [CrossRef]

26. Chmielewski, M.; Gieras, M.; Niszczota, P. Fuel-Water emulsion impact on miniature gas turbine pollutant emission. In Proceedings of the E3S Web of Conferences, Warsaw, Poland, 3–6 December 2019; EDP Sciences: Les Ulis, France, 2019; Volume 137, p. 01046.
27. Chmielewski, M.; Niszczota, P.; Gieras, M. Combustion efficiency of fuel-water emulsion in a small gas turbine. *Energy* **2020**, *211*, 118961. [CrossRef]
28. Park, J.; Nguyen, T.H.; Joung, D.; Huh, K.Y.; Lee, M.C. Prediction of NO_x and CO Emissions from an Industrial Lean-Premixed Gas Turbine Combustor Using a Chemical Reactor Network Model. *Energy Fuels* **2013**, *27*, 1643–1651. [CrossRef]
29. Łapucha, R. *Komory Spalania Silników Turbinowo-Odrzutowych: Procesy, Obliczenia, Badania*; Wydawnictwa Naukowe Instytutu Lotnictwa: Warsaw, Poland, 2004; pp. 117–152. ISBN 83-915995-8-2.
30. Mann, M.; Jainski, C.; Euler, M.; Böhm, B.; Dreizler, A. Transient flame-wall interactions: Experimental analysis using spectroscopic temperature and CO concentration measurements. *Combust. Flame* **2014**, *161*, 2371–2386. [CrossRef]
31. Gieras, M.; Stańkowski, T. Computational study of an aerodynamic flow through a micro-turbine engine combustor. *J. Power Technol.* **2012**, *92*, 68–79.
32. Gonzalez, C.A.; Wong, K.C.; Armfield, S. A computational study of the influence of the injection characteristics on micro-turbine combustion. In Proceedings of the 16th Australasian Fluid Mechanics Conference Crown Plaza, Gold Coast, Australia, 2–7 December 2007.
33. Chmielewski, M.; Gieras, M. Study of combustion efficiency and pollutant emissions in a miniature gas turbine with the combustion chamber of variable geometry. *Rynek Energii* **2015**, *4*, 103–109.
34. Chmielewski, M.; Gieras, M. Impact of variable geometry combustor on performance and emissions from miniature gas turbine engine. *J. Energy Inst.* **2017**, *90*, 257–264. [CrossRef]
35. Jing, W.; Roberts, W.L.; Fang, T. Spray combustion of Jet-A and diesel fuels in a constant volume combustion chamber. *Energy Convers. Manag.* **2015**, *89*, 525–540. [CrossRef]
36. Buschmann, A.; Dinkelacker, F.; Schäfer, T.; Wolfrum, J.; Schäfer, M. Measurement of the instantaneous detailed flame structure in turbulent premixed combustion. *Symp. Int. Combust.* **1996**, *26*, 437–445. [CrossRef]
37. Lefebvre, A.H.; Ballal, D.R. *Gas Turbine Combustion: Alternative Fuels and Emissions*; CRC Press: Boca Raton, FL, USA, 2010.
38. Gieras, M. *Komory Spalania Silników Turbinowych: Organizacja Procesu Spalania*, 1st ed.; Oficyna Wydawnicza Politechniki Warszawskiej: Warsaw, Poland, 2010; pp. 81–84. ISBN 978-83-7207-864-3.
39. Law, C.K. A Model for the Combustion of Oil/Water Emulsion Droplets. *Combust. Sci. Technol.* **1977**, *17*, 29–38. [CrossRef]
40. Gumus, M.; Sayin, C.; Canakci, M. The impact of fuel injection pressure on the exhaust emissions of a direct injection diesel engine fueled with biodiesel–diesel fuel blends. *Fuel* **2012**, *95*, 486–494. [CrossRef]
41. Chen, P.-C.; Wang, W.-C.; Roberts, W.L.; Fang, T. Spray and atomization of diesel fuel and its alternatives from a single-hole injector using a common rail fuel injection system. *Fuel* **2013**, *103*, 850–861. [CrossRef]
42. Kadota, T.; Yamasaki, H. Recent advances in the combustion of water fuel emulsion. *Prog. Energy Combust. Sci.* **2002**, *28*, 385–404. [CrossRef]
43. Rao, D.C.K.; Karmakar, S.; Som, S.K. Puffing and Micro-Explosion Behavior in Combustion of Butanol/Jet A-1 and Acetone-Butanol-Ethanol (A-B-E)/Jet A-1 Fuel Droplets. *Combust. Sci. Technol.* **2017**, *189*, 1796–1812. [CrossRef]
44. Rodzewicz, R.; Gieras, M. Numerical investigation of heat transfer in fuel-water emulsion droplet. *Arch. Combust.* **2018**, *38*, 1–10.
45. Watanabe, H.; Suzuki, Y.; Harada, T.; Matsushita, Y.; Aoki, H.; Miura, T. An experimental investigation of the breakup characteristics of secondary atomization of emulsified fuel droplet. *Energy* **2010**, *35*, 806–813. [CrossRef]